Taylor & Francis
Taylor & Francis Group

INVITED ARTICLE

Structural, energetic and vibrational properties of some van der Waals complexes of CO_2, OCS and OCSe

Ponnadurai Ramasami[a] and Thomas A. Ford[b,*]

aDepartment of Chemistry, Faculty of Science, Computational Chemistry Group, University of Mauritius, Réduit, Mauritius; bSchool of Chemistry and Physics, University of KwaZulu-Natal, Durban, South Africa

As part of a study of the properties of some chalcogen-bonded complexes with NH_3, H_2O, PH_3 and H_2S, we have investigated the oxygen-bound species containing CO_2, OCS and OCSe by means of molecular orbital calculations at the *ab initio* level. The structures of the NH_3, H_2O and PH_3 complexes are all similar, with a primary C...X interaction (X = N, O, P) and one of the hydrogen atoms approaching an oxygen atom in a weak secondary attraction. The H_2S complexes show a greater variety of alternative structures. The changes in the monomer geometrical parameters, the interaction energies and the harmonic vibrational spectra vary in general in a systematic way as the acid and the base are changed. Deviations from this systematic behaviour have been rationalised.

Keywords: *ab initio* calculations; molecular complexes; molecular structures; interaction energies; vibrational spectra

1. Introduction

We have previously presented the results of our *ab initio* calculations of the properties of the van der Waals complexes formed between the related Lewis acids – carbon dioxide, carbonyl sulphide, carbon disulphide and nitrous oxide – and the electron donors – nitrogen [1], ozone [2], carbon monoxide [3] and sulphur dioxide [4]. We found that the structures were, by and large, similar to one another, with a lone pair orbital of the base interacting with the carbon or the central nitrogen atom of the electron acceptor. In the same way, we have reported similar results for the complexes of the series of electron donors, ammonia, water, hydrogen fluoride, phosphine, hydrogen sulphide and hydrogen chloride, with the Lewis acids, boron trifluoride [5–8], sulphur dioxide [9], silicon tetrafluoride [10], fluoroacetylene [11], the halogens and interhalogens, F_2, Cl_2, Br_2, ClF, BrF and BrCl [12], and fluoroform [13,14]. In these cases, the major interaction was the donation of a lone pair of electrons of the base to a vacant orbital located mainly on the B, S or Si atom [5–10], to a σ^*(CH) antibonding orbital [11,13,14] or to a σ^*(XY) orbital (X, Y = F, Cl, Br) [12]. The interest in the properties of the complexes with fluoroacetylene and fluoroform [11,13,14] was related to a search for evidence for blue-shifting hydrogen-bonding interactions, and in those with the halogens and interhalogens [12] to detecting halogen-bonding interactions, and to compare the properties of these unusual non-covalent interactions with those of the more conventional hydrogen bonds. A further example of a non-covalent interaction

which has generated a good deal of interest recently is the chalcogen bond [15,16]. We are now extending our theoretical studies to the NH_3, H_2O, PH_3 and H_2S family on the one hand, and the CO_2, CS_2, CSe_2, OCS, OCSe and SCSe series on the other, in an attempt to identify the presence of chalcogen-bonded interactions among the various pairs of molecules in these series. In this first paper, as a calibration data-set, we concentrate on the oxygen-containing Lewis acids, CO_2, OCS and OCSe, in which a conventional non-covalent interaction is likely to be observed, before going on to examine the associated species bound through the sulphur and selenium atoms, where the probability of detecting S...X and Se...X interactions (X = N, O, P, S) is higher. Our focus will be mainly on the structures, the interaction energies and the vibrational spectra of the various aggregates, and we shall examine the ways in which these properties vary as the acid and the base are systematically changed, and how they are linked to one another.

Of the possible binary combinations of molecules which may be permuted from these two sets, the $CO_2 \cdot H_2O$ complex has been by far the most thoroughly studied, both experimentally, in the gas phase [17–19] and in cryogenic matrices [20–24], and theoretically [25–41]. Even so, its structure is far from unequivocally settled. In addition, the gas phase experimental studies of $OCS \cdot H_2O$ [42], $CS_2 \cdot H_2O$ [43], $CO_2 \cdot H_2S$ [44], $CO_2 \cdot NH_3$ [45,46] and $OCS \cdot NH_3$ [46], the matrix isolation infrared spectra of $CO_2 \cdot NH_3$ [47,48] and theoretical computations on $OCS \cdot H_2O$ [40,49], $CS_2 \cdot H_2O$ [40], $CO_2 \cdot H_2S$ [41] and $CO_2 \cdot NH_3$ [29,48,50]

---

*Corresponding author. Email: ford@ukzn.ac.za
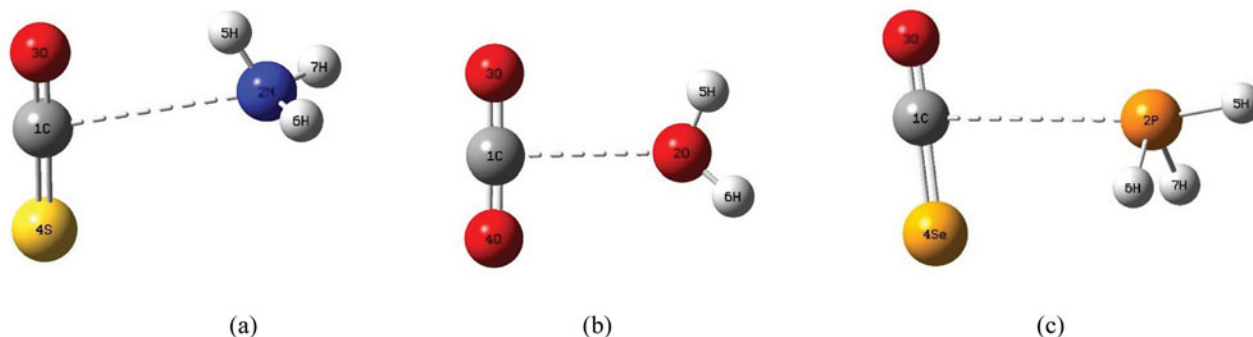
Figure 1. Optimised geometries of the (a) OCS·NH$_3$, (b) CO$_2$·H$_2$O and (c) OCSe·PH$_3$ complexes.

have appeared. We have found no reports of relevant complexes containing PH$_3$ or OCSe.

2. Computational details

The calculations were carried out using the Gaussian-09 program [51] at the second-order level of Møller–Plesset perturbation theory (MP2) [52] and with Dunning's augmented correlation-consistent polarised valence triple-zeta basis set (aug-cc-pVTZ) [53–57]. The tight convergence criterion was applied [51], and genuine minima on the potential energy surfaces were confirmed by vibrational analyses. In some cases, a number of possible structures for each complex were examined, but the alternatives were found to be either saddle points or local minima. The interaction energies were computed and corrected for basis set superposition error (BSSE) [58] using the full counterpoise procedure [59], and for vibrational zero-point energy differences.

3. Results and discussion

3.1. Molecular structures

The structures of the complexes containing ammonia, water and phosphine were characterised by a formal C...X interaction (X = N, O, P), in an essentially T-shaped

configuration, with one XH bond approaching the oxygen atom of OCY (Y = O, S, Se), tilted to a greater or lesser extent towards the CO bond. Structures of three examples of these complexes are illustrated in Figure 1. The complexes containing hydrogen sulphide yielded a far greater variety of stationary points; Figure 2 shows the optimised structures of the preferred isomers. The gas phase molecular beam electric resonance rotational spectrum of CO$_2$·NH$_3$ is interpreted in terms of a T-shaped structure with the N...CO$_2$ fragment having local C_{2v} symmetry, an N...C distance of 298.75 pm and a bending angle of the NH$_3$ sub-unit of 22.71° relative to the N...C axis [45,46]. This structure is consistent with the conclusions of Reed et al. [29], Jönsson and Nelander [48] and Amos and co-workers [50], based on their ab initio studies, with C...N bond lengths of 291, 286 and 295.0 pm, respectively. Fraser et al., in their microwave and infrared study of OCS·NH$_3$ [46], concluded that its structure was similar to that of CO$_2$·NH$_3$.

A number of rotational gas phase studies of CO$_2$·H$_2$O also proposed a planar T-shaped structure of this adduct, with C_{2v} symmetry and C...O distances of 283.6 pm [17] and 279.17 pm [18], although the spectra are complicated by rotation tunnelling splitting and the effect of wide amplitude motions [17–19]. A large number of theoretical studies, at levels ranging from self-consistent field (SCF) [30], Møller-Plesset perturbation theory at second order (MP2)
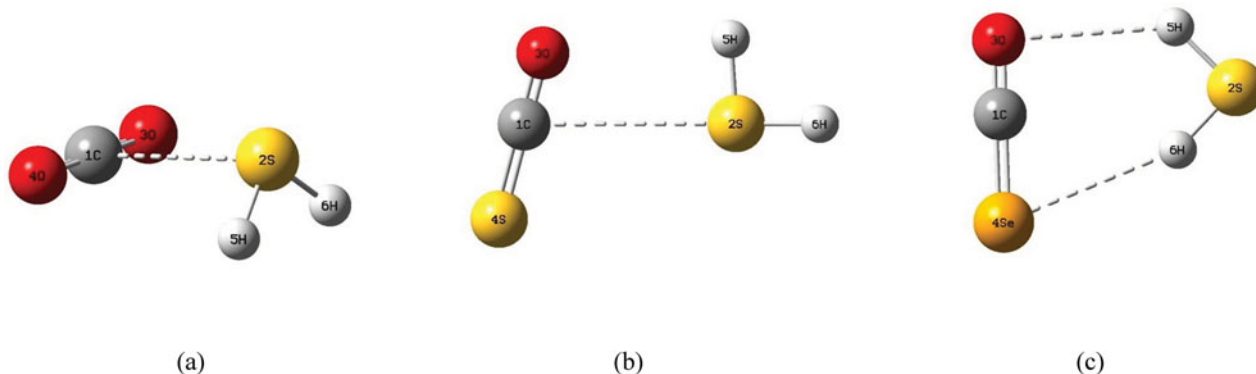

Figure 2. Optimised geometries of the (a) CO$_2$·H$_2$S, (b) OCS·H$_2$S and (c) OCSe·H$_2$S complexes.

Table 1. Changes in the intramolecular bond lengths and angles of the complexes of NH_3, H_2O, PH_3 and H_2S with CO_2, OCS and OCSe. See Figures 1 and 2 for numbering of the atoms.

Complex	Parameter	Change	Complex	Parameter	Change	Complex	Parameter	Change
$CO_2 \cdot NH_3$	r(C1O3), r(C1O4)/pm	0.006	OCS·NH_3	r(C1O3)/pm	0.091	OCSe·NH_3	r(C1O3)/pm	−0.321
	r(C1O4)/pm	−0.023		r(C1S4)/pm	−0.207		r(C1Se4)/pm	0.420
	∠O3C1O4/deg	−2.443		∠O3C1S4/deg	−0.870		∠O3C1Se4/deg	−1.359
	r(N2H5)/pm	0.048		r(N2H5)/pm	0.072		r(N2H5)/pm	0.064
	r(N2H6), r(N2H7)/pm	0.050		r(N2H6), r(N2H7)/pm	0.041		r(N2H6), r(N2H7)/pm	0.061
	∠H5N2H6, ∠H5N2H7/deg	0.003		∠H5N2H6, ∠H5N2H7/deg	0.016		∠H5N2H6, ∠H5N2H7/deg	0.185
	∠H6N2H7/deg	−0.263		∠H6N2H7/deg	−0.168		∠H6N2H7/deg	−0.439
$CO_2 \cdot H_2O$	r(C1O3)/pm	0.020	OCS·H_2O	r(C1O3)/pm	0.204	OCSe·H_2O	r(C1O3)/pm	0.207
	r(C1O4)/pm	−0.086		r(C1S4)/pm	−0.364		r(C1Se4)/pm	−0.427
	∠O3C1O4/deg	−1.693		∠O3C1S4/deg	−0.463		∠O3C1Se4/deg	−0.375
	r(O2H5)/pm	0.036		r(O2H5)/pm	0.101		r(O2H5)/pm	0.097
	r(O2H6)/pm	0.011		r(O2H6)/pm	0.007		r(O2H6)/pm	0.013
	∠H5O2H6/deg	0.510		∠H5O2H6/deg	0.441		∠H5O2H6/deg	0.400
$CO_2 \cdot PH_3$	r(C1O3)/pm	−0.090	OCS·PH_3	r(C1O3)/pm	−0.126	OCSe·PH_3	r(C1O3)/pm	−0.139
	r(C1O4)/pm	0.010		r(C1S4)/pm	0.186		r(C1Se4)/pm	0.196
	∠O3C1O4/deg	−0.572		∠O3C1S4/deg	−0.332		∠O3C1Se4/deg	−0.313
	r(P2H5)/pm	−0.068		r(P2H5)/pm	0.065		r(P2H5)/pm	0.103
	r(P2H6), r(P2H7)/pm	−0.062		r(P2H6), r(P2H7)/pm	−0.006		r(P2H6), r(P2H7)/pm	−0.014
	∠H5P2H6, ∠H5P2H7/deg	0.469		∠H5P2H6, ∠H5P2H7/deg	0.320		∠H5P2H6, ∠H5P2H7/deg	0.374
	∠H6P2H7/deg	0.234		∠H6P2H7/deg	0.086		∠H6P2H7/deg	0.121
$CO_2 \cdot H_2S$	r(C1O3), r(C1O4)/pm	−0.002	OCS·H_2S	r(C1O3)/pm	0.128	OCSe·H_2S	r(C1O3)/pm	0.032
	∠O3C1O4/deg	−0.919		r(C1S4)/pm	−0.194		r(C1Se4)/pm	−0.028
	r(S2H5), r(S2H6)/pm	0.025		∠O3C1S4/deg	−0.188		∠O3C1Se4/deg	−0.659
	∠H5S2H6/deg	0.207		r(S2H5)/pm	−0.002		r(S2H5)/pm	0.107
				r(S2H6)/pm	0.038		r(S2H6)/pm	0.230
				∠H5S2H6/deg	0.442		∠H5S2H6/deg	−0.119

Table 2. Intermolecular geometries of the complexes of NH_3, H_2O, PH_3, and H_2S with CO_2, OCS and OCSe. See Figures 1 and 2 for numbering of the atoms.

Complex	Parameter	Value	Complex	Parameter	Value	Complex	Parameter	Value
$CO_2 \cdot NH_3$	r(C1...N2)/pm	293.70	OCS·NH_3	r(C1...N2)/pm	321.46	OCSe·NH_3	r(C1...N2)/pm	316.58
	∠O3C1...N2/deg	90.54		∠O3C1...N2/deg	77.08		∠O3C1...N2/deg	93.09
	∠O4C1...N2/deg	91.90		∠S4C1...N2/deg	103.79		∠Se4C1...N2/deg	88.27
	∠C1...N2H5/deg	109.27		∠C1...N2H5/deg	74.32		∠C1...N2H5/deg	154.54
	∠C1...N2H6, ∠C1...N2H7/deg	113.54		∠C1...N2H6, ∠C1...N2H7/deg	125.58		∠C1...N2H6, ∠C1...N2H7/deg	87.82
$CO_2 \cdot H_2O$	r(C1...O2)/pm	277.41	OCS·H_2O	r(C1...O2)/pm	306.52	OCSe·H_2O	r(C1...O2)/pm	308.06
	∠O3C1...O2/deg	87.97		∠O3C1...O2/deg	72.59		∠O3C1...O2/deg	71.92
	∠O4C1...O2/deg	93.72		∠S4C1...O2/deg	107.87		∠Se4C1...O2/deg	108.45
	∠C1...O2H5/deg	115.86		∠C1...O2H5/deg	72.00		∠C1...O2H5/deg	72.12
	∠C1...O2H6/deg	139.52		∠C1...O2H6/deg	176.55		∠C1...O2H6/deg	176.63
$CO_2 \cdot PH_3$	r(C1...P2)/pm	346.88	OCS·PH_3	r(C1...P2)/pm	356.65	OCSe·PH_3	r(C1...P2)/pm	355.72
	∠O3C1...P2/deg	103.27		∠O3C1...P2/deg	98.17		∠O3C1...P2/deg	97.80
	∠O4C1...P2/deg	77.31		∠S4C1...P2/deg	82.16		∠Se4C1...P2/deg	82.51
	∠C1...P2H5/deg	158.43		∠C1...P2H5/deg	170.70		∠C1...P2H5/deg	169.54
	∠C1...P2H6, ∠C1...P2H7/deg	100.55		∠C1...P2H6, ∠C1...P2H7/deg	92.41		∠C1...P2H6, ∠C1...P2H7/deg	93.14
$CO_2 \cdot H_2S$	r(C1...S2)/pm	339.80	OCS·H_2S	r(C1...S2)/pm	338.97	OCSe·H_2S	r(C1...S2)/pm	371.41
	∠O3C1...S2/deg	90.46		∠O3C1...S2/deg	73.54		r(O3...H5)/pm	277.22
	∠O4C1...S2/deg	90.46		∠S4C1...S2/deg	106.28		r(Se4...H6)/pm	295.83
	∠C1...S2H5/deg	95.81		∠C1...S2H5/deg	87.75		∠S2H5...O3/deg	130.83
	∠C1...S2H6/deg	95.81		∠C1...S2H6/deg	179.58		∠S2H6...Se4/deg	155.61
							∠S2...C1O3/deg	84.46
							∠S2...C1Se4/deg	94.88
							∠C1...S2H5/deg	51.56
							∠C1...S2H6/deg	40.55
							∠C1O3...H5/deg	93.15
							∠C1Se4...H6/deg	68.97

Table 3.   Interaction energies of the complexes of NH_3, H_2O, PH_3 and H_2S with CO_2, OCS and OCSe.

Complex	Interaction energy/kJ mol^{-1}		
	Uncorrected	Corrected for BSSE only	Corrected for BSSE and ΔE_o
$CO_2 \cdot NH_3$	−12.620	−11.545	−9.225
$CO_2 \cdot H_2O$	−12.004	−10.838	−6.847
$CO_2 \cdot PH_3$	−6.997	−5.702	−4.796
$CO_2 \cdot H_2S$	−7.960	−6.816	−4.980
$OCS \cdot NH_3$	−8.283	−7.029	−5.730
$OCS \cdot H_2O$	−9.005	−7.629	−5.658
$OCS \cdot PH_3$	−7.980	−6.183	−4.511
$OCS \cdot H_2S$	−7.766	−6.259	−4.582
$OCSe \cdot NH_3$	−9.520	−6.445	−4.477
$OCSe \cdot H_2O$	−9.075	−6.994	−4.233
$OCSe \cdot PH_3$	−10.000	−6.493	−4.249
$OCSe \cdot H_2S$	−10.036	−6.122	−3.827

Figure 3.   Plots of the interaction energies of the complexes versus the quadrupole moments of the electron acceptors.

[29,32–34,37,38,41] and fourth order (MP4) [39] to coupled cluster with singles, doubles and perturbative triples (CCSD(T)) [40], as well as density functional theory (DFT) [35], and employing a variety of basis sets, are in agreement with these findings, while Nguyen and Ha [26] determined that the planar form was more stable than the corresponding perpendicular C_{2v} structure. The computed C...O separations lie in a range from 250.2 pm (DFT/Vosko,Wilk,Nusair (VWN64)) [35] to 290.6 pm (MP4/spd) [39]. Damewood *et al*. [32], Cox and co-workers [34,36] and Altmann and Ford [41] examined a number of possible configurations and concluded that the potential energy surface was so shallow that facile interconversion among the various competing structures was possible. The present result indicates that the C_s structure is the true global minimum, and that the C_{2v} species is simply a vibrationally averaged structure, in agreement with Abashkin *et al*. [35].

The experimental gas phase results of Rice *et al*. [44] on $CO_2 \cdot H_2S$ established that the H_2S plane was essentially perpendicular (92°) to the heavy atom plane, and the centre-of-mass separation was 349.8 pm, consistent with our present results and with those of Altmann and Ford [41], using the same computational approach. The microwave rotational spectrum of $OCS \cdot H_2O$ [42] represents the first point of departure of our computed structures from those determined experimentally. Tatamitani and Ogata [42] found the structure of this adduct to be planar, of C_{2v} symmetry, but with an S...O interaction. This was the structure found theoretically by Garden *et al*. [40], although the work of Wojcik and colleagues [49], using a smaller basis set than ours, confirms our findings. In this work, we have examined only those complexes bound through an oxygen atom, so we concede

Table 4.   Computed and experimental vibrational spectra of the $CO_2 \cdot NH_3$ complex.

Symmetry	Mode	Approximate description	ν(calc.)/cm^{-1} (this work)	ν(expt.)/cm^{-1}[47]	ν(calc.)/ ν(expt.)
a'	ν_1	$\nu_a(NH_3)$	3644.0	–	–
	ν_2	$\nu_s(NH_3)$	3498.0	3326.9	1.05
	ν_3	$\nu_a(CO_2)$	2401.8	2282.8	1.05
	ν_4	$\delta_a(NH_3)$	1668.4	1623.7	1.03
	ν_5	$\nu_s(CO_2)$	1327.6	–	–
	ν_6	$\delta_s(NH_3)$	1062.5	1001.9	1.06
	ν_7	$\delta(CO_2)$	636.7	662.3	0.96
	ν_8	$\rho(NH_3)$	189.9	–	–
	ν_9	$\nu(C...N)$	105.0	–	–
	ν_{10}	Antigeared libration	42.4	–	–
a''	ν_{11}	$\nu_a(NH_3)$	3643.0	–	–
	ν_{12}	$\delta_a(NH_3)$	1668.3	1621.7	1.03
	ν_{13}	$\gamma(CO_2)$	664.7	662.3	1.00
	ν_{14}	$\rho(NH_3)$	135.7	–	–
	ν_{15}	$\tau(NH_3)$	7.1	–	–

that the structure determined here may be a local minimum on the potential energy surface, and that the true global minimum is the chalcogen-bonded $OCS...OH_2$ form. We will be exploring this and similar possible complexes in a future publication.

The changes to the bond lengths and angles of the monomers constituting each of the complexes studied here are collected in Table 1. These changes are minimal, suggesting that the complexes are all weakly bound. The bond lengths of the base fragments tend to increase slightly, except for the PH bond lengths, confirming that PH_3 occupies a unique position among the electron donors considered here, on account of the reversal of the polarity of the PH bond relative to NH, OH and SH, as we have pointed out before [10–14]. The HOH, HPH and HSH angles, as well as the HNH angles involving the in-plane NH bond, increase on complexation accompanied by a contraction in the case of the HNH angles associated with the out-of-plane NH bonds. The bound CO bond lengths of the acids mostly increase, except for the PH_3 complexes, as observed above, while the reverse is true for the non-bound CO and the CS and CSe bonds. The changes in the OCY bond angles are generally greater for the complexes with NH_3 and H_2O, and the OCO angle appears to be the most sensitive to complexation, but since these changes are all small some circumspection is required in the interpretation of these numbers.

Table 2 lists the intermolecular geometries of the complexes. Our C...X separations compare reasonably well with those experimental values which are available [17,18,44–46], and with other reported theoretical results, depending on the levels of theory and basis sets used in each case [29,30,32–35,37–41]. The C...X separations roughly follow the generalisations $CO_2 < OCS \approx OCSe$ and $NH_3 \approx H_2O < PH_3 \approx H_2S$. The C...XH angles are a measure of the extent of interaction between the in-plane XH bond and the CO bond. The C...PH angles are substantially larger than the others, as a result of the repulsion between the negatively charged O and H atoms, arising from the reversal of the polarity of the PH bond referred to above. The $OCSe·H_2S$ complex is a unique case, on account of the cyclic doubly hydrogen-bonded structure of this species.

3.2. Interaction energies

The interaction energies of the 12 complexes, corrected for both BSSE and zero-point energy differences, are collected in Table 3. As predicted by the minimal perturbations of the intramolecular bond lengths and angles mentioned above, the magnitudes of these binding energies are also consistent with very weak interactions. Previously reported interaction energies cover a very wide range, indicative of the use of several levels of theory and basis sets (-15.77 [29] to -29.29 kJ mol^{-1} [48] for $CO_2·NH_3$, -7.55 [41] to -25.7 kJ mol^{-1} [25] for $CO_2·H_2O$, -4.65 kJ mol^{-1} [41] for $CO_2·H_2S$ and -5.44 [40] to -11.51 kJ mol^{-1} [49] for

Table 5. Computed and experimental vibrational spectra of the $CO_2·H_2O$ complex.

Symmetry	Mode	ν(calc.)/cm^{-1} (this work)	ν(expt.)/cm^{-1} [20]	ν(calc.)/ ν(expt.) [20]	ν(expt.)/ cm^{-1} [21,22]	ν(calc.)/ ν(expt.) [21,22]	ν(expt.)/ cm^{-1} [23]	ν(calc.)/ ν(expt.) [23]	ν(expt.)/ cm^{-1} [24]	ν(calc.)/ ν(expt.) [24]
a'	ν_1	3944.6	3724.8	1.06	3731.3 3730.0	1.06 1.06	3725.5 3724.1	1.06 1.06	–	–
	ν_2	3818.5	3632.1	1.05	3633.5	1.05	3632.4 3631.7	1.05 1.05	3632.0 3632.7	1.05 1.05
	ν_3	2404.4	2351	1.02	2344.3 2341.9	1.03 1.03	2351.0	1.02	2351.1	1.02
	ν_4	1626.5	1598.1	1.02	1600.7	1.02	1598.4	1.02	–	–
	ν_5	1328.6	1384.5	0.96	–	–	–	–	1384.8	0.96
	ν_6	648.8	656.3	0.99	654.2	0.99	656.3	0.99	656.4	0.99
	ν_7	166.0	–	–	–	–	–	–	–	–
	ν_8	110.8	–	–	–	–	–	–	–	–
	ν_9	10.6	–	–	–	–	–	–	–	–
a''	ν_{10}	662.6	665.3	1.00	666.9	0.99	665.2	0.97	665.3	1.00
	ν_{11}	156.2	–	–	–	–	–	–	–	–
	ν_{12}	93.3	–	–	–	–	–	–	–	–

Approximate description:
ν_1: $\nu_a(H_2O)$; ν_2: $\nu_s(H_2O)$; ν_3: $\nu_a(CO_2)$; ν_4: $\delta(H_2O)$; ν_5: $\nu_s(CO_2)$; ν_6: $\delta(CO_2)$; ν_7: $\rho(H_2O)$; ν_8: $\nu(C...O)$; ν_9: Antigeared libration; ν_{10}: $\gamma(CO_2)$; ν_{11}: $tw(H_2O)$; ν_{12}: $\omega(H_2O)$

Table 6. Computed complex-monomer wavenumber shifts of the complexes of NH_3, H_2O, PH_3 and H_2S with CO_2, OCS and OCSe.

Complex	Monomer	Mode	Shift/cm⁻¹	Complex	Monomer	Mode	Shift/cm⁻¹	Complex	Monomer	Mode	Shift/cm⁻¹
$CO_2 \cdot NH_3$	CO_2	$\nu_s(CO_2)$	1.8	OCS·NH_3	OCS	$\nu(CO)$	−0.3	OCSe·NH_3	OCSe	$\nu(CO)$	10.1
		$\delta(CO_2)(a')$	−22.3			$\delta(OCS)(a')$	−8.9			$\delta(OCSe)(a')$	−12.1
		$\delta(CO_2)(a'')$	5.7			$\delta(OCS)(a'')$	2.4			$\delta(OCSe)(a'')$	0.4
		$\nu_a(CO_2)$	0.4			$\nu(CS)$	3.7			$\nu(CSe)$	−5.8
	NH_3	$\nu_s(NH_3)$	−4.9		NH_3	$\nu_s(NH_3)$	−6.2		NH_3	$\nu_s(NH_3)$	−8.3
		$\delta_s(NH_3)$	25.1			$\delta_s(NH_3)$	12.5			$\delta_s(NH_3)$	12.8
		$\nu_a(NH_3)(a')$	−5.9			$\nu_a(NH_3)(a')$	−7.7			$\nu_a(NH_3)(a')$	−7.4
		$\nu_a(NH_3)(a'')$	−6.9			$\nu_a(NH_3)(a'')$	−5.3			$\nu_a(NH_3)(a'')$	−8.7
		$\delta_a(NH_3)(a')$	−0.5			$\delta_a(NH_3)(a')$	−1.7			$\delta_a(NH_3)(a')$	−7.2
		$\delta_a(NH_3)(a'')$	−0.6			$\delta_a(NH_3)(a'')$	1.3			$\delta_a(NH_3)(a'')$	−5.3
$CO_2.H_2O$	CO_2	$\nu_s(CO_2)$	2.8	$OCS.H_2O$	OCS	$\nu(CO)$	−1.4	$OCSe.H_2O$	OCSe	$\nu(CO)$	−2.4
		$\delta(CO_2)(a')$	−10.2			$\delta(OCS)(a')$	−1.2			$\delta(OCSe)(a')$	−0.6
		$\delta(CO_2)(a'')$	3.6			$\delta(OCS)(a'')$	1.0			$\delta(OCSe)(a'')$	1.4
		$\nu_a(CO_2)$	3.0			$\nu(CS)$	6.2			$\nu(CSe)$	6.8
	H_2O	$\nu_s(H_2O)$	−3.4		H_2O	$\nu_s(H_2O)$	−9.7		H_2O	$\nu_s(H_2O)$	−9.7
		$\delta(H_2O)$	−1.8			$\delta(H_2O)$	−6.5			$\delta(H_2O)$	−6.1
		$\nu_a(H_2O)$	−3.1			$\nu_a(H_2O)$	−8.5			$\nu_a(H_2O)$	−8.7
$CO_2.PH_3$	CO_2	$\nu_s(CO_2)$	0.1	$OCS.PH_3$	OCS	$\nu(CO)$	2.3	$OCSe.PH_3$	OCSe	$\nu(CO)$	3.4
		$\delta(CO_2)(a')$	−10.6			$\delta(OCS)(a')$	−7.0			$\delta(OCSe)(a')$	−7.0
		$\delta(CO_2)(a'')$	−0.2			$\delta(OCS)(a'')$	−0.9			$\delta(OCSe)(a'')$	−1.1
		$\nu_a(CO_2)$	−1.0			$\nu(CS)$	−2.7			$\nu(CSe)$	−2.6
	PH_3	$\nu_s(PH_3)$	3.8		PH_3	$\nu_s(PH_3)$	−2.1		PH_3	$\nu_s(PH_3)$	−3.8
		$\delta_s(PH_3)$	−1.8			$\delta_s(PH_3)$	−2.1			$\delta_s(PH_3)$	−2.8
		$\nu_a(PH_3)(a')$	5.3			$\nu_a(PH_3)(a')$	−1.9			$\nu_a(PH_3)(a')$	−3.1
		$\nu_a(PH_3)(a'')$	4.5			$\nu_a(PH_3)(a'')$	0.5			$\nu_a(PH_3)(a'')$	0.8
		$\delta_a(PH_3)(a')$	−2.2			$\delta_a(PH_3)(a')$	−4.0			$\delta_a(PH_3)(a')$	−5.2
		$\delta_a(PH_3)(a'')$	−1.0			$\delta_a(PH_3)(a'')$	−1.3			$\delta_a(PH_3)(a'')$	−1.4
$CO_2.H_2S$	CO_2	$\nu_s(CO_2)$	0.7	$OCS.H_2S$	OCS	$\nu(CO)$	−2.4	$OCSe.H_2S$	OCSe	$\nu(CO)$	−1.9
		$\delta(CO_2)(ip)$[a]	−13.0			$\delta(OCS)(a')$	−2.2			$\delta(OCSe)(a')$	−2.0
		$\delta(CO_2)(op)$[b]	1.0			$\delta(OCS)(a'')$	−1.1			$\delta(OCSe)(a'')$	0.5
		$\nu_a(CO_2)$	0.1			$\nu(CS)$	3.1			$\nu(CSe)$	0.8
	H_2S	$\nu_s(H_2S)$	−1.9		H_2S	$\nu_s(H_2S)$	−1.7		H_2S	$\nu_s(H_2S)$	−19.2
		$\delta(H_2S)$	−0.6			$\delta(H_2S)$	−4.3			$\delta(H_2S)$	4.7
		$\nu_a(H_2S)$	−1.6			$\nu_a(H_2S)$	−0.7			$\nu_a(H_2S)$	−14.1

[a]Bending in the S...CO_2 plane.
[b]Bending perpendicular to the S...CO_2 plane.

Table 7. Experimental complex-monomer wavenumber shifts of the $CO_2 \cdot NH_3$ and $CO_2 \cdot H_2O$ complexes.

Complex	Monomer	Mode	Wavenumber shift/cm^{-1}				
			[47]	[20]	[21,22]	[23]	[24]
$CO_2 \cdot NH_3$	CO_2	$\nu_s(CO_2)$	–				
		$\delta(CO_2)(a')$	−12.7				
		$\delta(CO_2)(a'')$	4.1				
		$\nu_a(CO_2)$	−1.0				
	NH_3	$\nu_s(NH_3)$	−3.1				
		$\delta_s(NH_3)$	32.7				
		$\nu_a(NH_3)(a')$	–				
		$\nu_a(NH_3)(a'')$	–				
		$\delta_a(NH_3)(a')$	−7.0				
		$\delta_a(NH_3)(a'')$	3.5				
$CO_2 \cdot H_2O$	CO_2	$\nu_s(CO_2)$		–	–	–	–
		$\delta(CO_2)(a')$		3.0	3.0	2.9	3.1
		$\delta(CO_2)(a'')$		−6.0	−9.8	−6.0	−5.8
		$\nu_a(CO_2)$		2.4	4.8, 2.4	2.0	2.6
	H_2O	$\nu_s(H_2O)$		−2.3	−3.2	−2.5, −3.2	−2.7, −2.0
		$\delta(H_2O)$		0.9	9.1	1.4	–
		$\nu_a(H_2O)$		−1.9	−1.0, −2.3	−1.9, −3.3	–

$OCS \cdot H_2O$). The upper bounds of the various ranges can usually be attributed to the neglect of BSSE. The overall trend in the strength of interaction is $NH_3 > H_2O > PH_3 \approx H_2S$, for all three electron acceptors. For complexes of the type described here, it may be anticipated that the major source of the interaction energy is the electrostatic component. We have not attempted to dissect the total interaction energies into the attractive electrostatic, charge transfer, polarisation and dispersion contributions, nor the repulsive Pauli exchange constituent. In the absence of a permanent dipole moment in the case of CO_2, the most probable main source of electrostatic attraction which is common to all the complexes is a dipole–quadrupole interaction. Values of the molecular quadrupole moments of CO_2, OCS and OCSe are available (−14.31, −0.984 and 4.442 × 10^{-40} C m^2 for CO_2, OCS [60] and OCSe [61]). As the quadrupole moment changes sign as O is replaced by S and then Se, and the negative poles change from the axial positions in CO_2 and OCS to equatorial in OCSe, the computed interaction energies diminish regularly, as shown in Figure 3. Since all the interaction energies are small, the difference between the PH_3 and H_2S complex properties barely register, except to distinguish them from those of the NH_3 and H_2O adducts. In any case, it is well known that the properties of complexes of second- and third-row molecules behave differently from those of the first row.

Vibrational spectra

Our computed spectrum of the $CO_2 \cdot NH_3$ complex is presented in Table 4. The matrix isolation infrared data of Fredin and Nelander in nitrogen [47] are consistent with this structure, and their data are also included in this table.

The calculated/experimental wavenumber ratios are well within the normal range for such comparisons at this level. Matrix isolation studies of the $CO_2 \cdot H_2O$ complex [20–24] favour the T-shaped structure over the hydrogen-bonded alternative, although Tso and Lee [21,22] have indicated that a second, hydrogen-bonded isomer may exist in oxygen matrices. While the earlier matrix investigations suggested that the $CO_2 \cdot H_2O$ complex possessed C_{2v} symmetry, more recent work, with the benefit of improved cryogenic technology and increased instrumental resolution, admits the possibility of a second C...O bonded species with C_s symmetry [23,24], a result we find to be compatible with
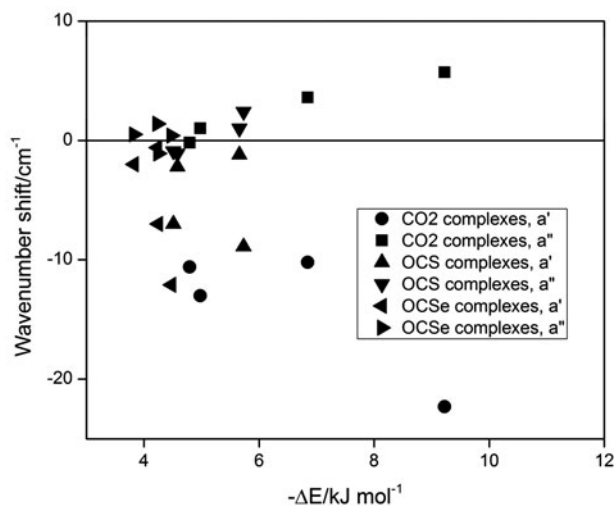

Figure 4. Plots of the OCY bending wavenumber shifts of the electron acceptors versus the complex interaction energies (Y = O, S, Se).

Table 8. Computed intermolecular wavenumbers of the complexes of NH$_3$, H$_2$O, PH$_3$ and H$_2$S with CO$_2$, OCS and OCSe.

Complex	Symmetry	Mode	Wavenumber/ cm^{-1}	Complex	Symmetry	Mode	Wavenumber/ cm^{-1}	Complex	Symmetry	Mode	Wavenumber/ cm^{-1}
CO$_2$·NH$_3$	a'	NH$_3$ rock / C...N stretch / Antigeared	189.8 / 105.0 / 42.4	OCS·NH$_3$	a'	NH$_3$ rock / C...N stretch / Antigeared	140.3 / 99.4 / 47.1	OCSe·NH$_3$	a'	NH$_3$ rock / C...N stretch / Antigeared	156.4 / 87.6 / 53.5
	a''	NH$_3$ rock / NH$_3$ torsion	135.7 / 7.1		a''	NH$_3$ rock / NH$_3$ torsion	73.9 / 21.3		a''	NH$_3$ rock / NH$_3$ torsion	110.7 / 49.5
CO$_2$·H$_2$O	a'	H$_2$O rock / C...O stretch / Antigeared	166.0 / 110.8 / 10.6	OCS.H$_2$O	a'	H$_2$O rock / C...O stretch / Antigeared	149.0 / 112.4 / 35.2	OCSe.H$_2$O	a'	H$_2$O rock / C...O stretch / Antigeared	141.4 / 108.0 / 31.0
	a''	H$_2$O twist / H$_2$O wag	156.2 / 93.3		a''	H$_2$O twist / H$_2$O wag	202.8 / 99.3		a''	H$_2$O twist / H$_2$O wag	196.2 / 105.7
CO$_2$·PH$_3$	a'	PH$_3$ rock / C...P stretch / Antigeared	123.7 / 57.6 / 25.3	OCS.PH$_3$	a'	PH$_3$ rock / C...P stretch / Antigeared	126.9 / 65.7 / 44.8	OCSe.PH$_3$	a'	PH$_3$ rock / C...P stretch / Antigeared	140.1 / 63.9 / 42.1
	a''	PH$_3$ rock / PH$_3$ torsion	76.2 / 37.5		a''	PH$_3$ rock / PH$_3$ torsion	117.4 / 17.8		a''	PH$_3$ rock / PH$_3$ torsion	134.1 / 19.4
CO$_2$·H$_2$S	a'	H$_2$S wag / C...S stretch	85.1 / 67.3	OCS.H$_2$S	a'	C...S stretch / H$_2$S rock	83.3 / 68.3	OCSe.H$_2$S	a'	H$_2$S rock / Intermonomer stretch	156.3 / 72.0
	a''	H$_2$S twist / H$_2$S rock / Antigeared	144.9 / 43.9 / 25.6		a''	Antigeared / H$_2$S twist / H$_2$S wag	35.7 / 142.3 / 45.5		a''	Antigeared / H$_2$S twist / H$_2$S wag	40.8 / 133.1 / 86.1

our present work. Our calculated wavenumbers and those determined experimentally in nitrogen [20,23,24] and oxygen [21,22] are listed in Table 5. Multiple entries for some of the observed bands are attributed to the presence of a second structure. Again, the calculated/experimental ratios are acceptable; only for the CO_2 bending vibrations are the predicted wavenumbers marginally lower than the observed ones. The computed complex-monomer wavenumber shifts for the 12 complexes are collected in Table 6, and their experimental counterparts [20–24,47] in Table 7. In line with the very small perturbations of the intramolecular geometrical parameters (Table 1) and low interaction energies (Table 3), the wavenumber shifts occurring on complexation are also minimal. By far, the most strongly affected modes are the bending vibrations. The symmetric NH_3 bending mode, ν_2, has long been regarded as a sensitive probe of the strength of interaction, particularly in the spectra of inorganic coordination compounds [62]. In this series of complexes, this mode undergoes the largest shift of any of the vibrations, characteristically to the blue. The calculated shift in $CO_2 \cdot NH_3$ of 25.1 cm^{-1} may be compared with the experimental value of 32.7 cm^{-1} [47], while those of $OCS \cdot NH_3$ and $OCSe \cdot NH_3$ are also large and to the blue (12.5 and 12.8 cm^{-1}, respectively). The remaining bending mode shifts are almost exclusively to lower wavenumber, but are substantially smaller. The exception is the H_2S bending mode of $OCSe \cdot H_2S$, ν_2, which shifts to the blue (4.7 cm^{-1}), as a result of the cyclic doubly hydrogen-bonded structure of this complex. For this complex, too, the H_2S stretching modes suffer uncharacteristically large (-19.2 and -14.1 cm^{-1}) shifts, typical of SH bonds engaged in hydrogen-bonded interactions. In those cases where the degeneracy of a linear bending mode is lifted on complexation, as in the CO_2, OCS and OCSe fragments, the resulting pairs of vibrations are typically perturbed with one large negative shift (the a' mode) and a smaller positive shift (the a'' mode). These computed shifts are fairly consistent with their experimental partners, and show a weak correlation with the interaction energies, as indicated in Figure 4.

Table 8 lists the computed wavenumbers of the intermolecular modes of the complexes. These modes fall into fairly well-defined characteristic ranges. For example, the intermolecular stretching vibrations for the NH_3 and H_2O complexes are fairly similar (80–110 cm^{-1}), and are about 50% higher than those for the PH_3 and H_2S adducts (50–80 cm^{-1}). Likewise, the NH_3 and PH_3 rocking modes are typically in the range 100–160 cm^{-1}, while the corresponding torsional modes are very low (<50 cm^{-1}). The H_2O vibrations are usually found in the order twisting > rocking > wagging, but apart from the consistently high wavenumbers of the twisting vibrations of the H_2S complexes, no such pattern is observed among the rocking and wagging vibrations of this group, due to the three different types of structure adopted by the H_2S complexes. These regular generalisations serve to confirm the internal consistency of the calculations.

4. Conclusions

The complexes of NH_3, H_2O and PH_3 with CO_2, OCS and OCSe all have qualitatively similar structures, while the H_2S complexes exhibit three different structural models. In those cases where comparison with experimentally determined structures is possible, our predictions are consistent with them. The interaction energies are all small, and the weak interactions are manifested in minimal perturbations of the monomer bond lengths and angles, although a dependence of the strengths of interaction on the quadrupole moments of the electron acceptors is observed. These small perturbations also extend to the vibrational spectra, where the bending wavenumber shifts of the linear electron acceptor molecules show a tentative correlation with the interaction energies. No evidence was found in these calculations for the existence of S or Se chalcogen-bound complexes, but a search for such adducts will be the subject of a forthcoming paper.

References

[1] M. Venayagamoorthy and T.A. Ford, J. Mol. Structure **565–566**, 399 (2001).
[2] M. Venayagamoorthy and T.A. Ford, J. Mol. Structure **651–653**, 223 (2003).
[3] M. Venayagamoorthy and T.A. Ford, J. Mol. Structure (Theochem) **717**, 111 (2005).
[4] M. Venayagamoorthy and T.A. Ford, South African J. Chem. **62**, 149 (2009).
[5] F. Gaffoor and T.A. Ford, Spectrochim. Acta, Part A **71**, 550 (2008).
[6] T.A. Ford, J. Phys. Chem. A **112**, 7296 (2008).
[7] G.A. Yeo and T.A. Ford, South African J. Chem. **59**, 129 (2006).
[8] G.A. Yeo and T.A. Ford, J. Mol. Structure (Theochem) **771**, 157 (2006).
[9] T.A. Ford, J. Mol. Structure, **924–926**, 466 (2009).
[10] P. Ramasami and T.A. Ford, J. Mol. Structure (Theochem) **940**, 50 (2010).
[11] P. Ramasami and T.A. Ford, Can. J. Chem. **88**, 716 (2010).
[12] P. Ramasami and T.A. Ford, Comput. Theor. Chem. **990**, 227 (2012).

[13] P. Ramasami and T.A. Ford, J. Mol. Structure **1023**, 163 (2012).

[14] P. Ramasami and T.A. Ford, J. Mol. Structure **1029**, 217 (2012).

[15] U. Adhikari and S. Scheiner, J. Phys. Chem. A **116**, 3487 (2012).

[16] S. Scheiner, Cryst. Eng. Commun. **15**, 3119 (2013).

[17] K.I. Peterson and W. Klemperer, J. Chem. Phys. **80**, 2439 (1984).

[18] P.A. Block, M.D. Marshall, L.G. Pedersen, and R.E. Miller, J. Chem. Phys. **96**, 7321 (1992).

[19] G. Columberg, A. Bauder, N. Heineking, W. Stahl, and J. Makarewicz, Mol. Phys. **93**, 215 (1998).

[20] L. Fredin, B. Nelander, and G. Ribbegard, Chem. Scripta **7**, 11 (1975).

[21] T.-L. Tso and E.K.C. Lee, J. Phys. Chem. **89**, 1612 (1985).

[22] T.-L. Tso and E.K.C. Lee, J. Phys. Chem. **89**, 1618 (1985).

[23] A. Schriver, L. Schriver-Mazzuoli, P. Chaquin, and E. Dumont, J. Phys. Chem. A **110**, 51 (2006).

[24] X. Zhang and S.P. Sander, J. Phys. Chem. A **115**, 9854 (2011).

[25] B. Jönsson, G. Karlström, and H. Wennerström, Chem. Phys. Lett. **30**, 58 (1975).

[26] M.T. Nguyen and T.-K. Ha, J. Am. Chem. Soc. **106**, 599 (1984).

[27] J.-Y. Liang and W.N. Lipscomb, J. Am. Chem. Soc. **108**, 5051 (1986).

[28] W.A. Sokalski, J. Mol. Structure **138**, 77 (1986).

[29] A.E. Reed, F. Weinhold, L.A. Curtiss, and D.J. Pochatko, J. Chem. Phys. **84**, 5687 (1986).

[30] G.J.B. Hurst, P.W. Fowler, A.J. Stone, and A.D. Buckingham, Int. J. Quantum Chem. **29**, 1223 (1986).

[31] M.T. Nguyen, A.J. Hegarty, and T.-K. Ha, J. Mol. Structure **150**, 319 (1987).

[32] J.A. Damewood, Jr., R.A. Kumpf, and W.C.F. Muhlbauer, J. Phys. Chem. **93**, 7640 (1989).

[33] J. Makarewicz, T.-K. Ha, and A. Bauder, J. Chem. Phys. **99**, 3694 (1993).

[34] A.J. Cox, T.A. Ford, and L. Glasser, in *Structures and Conformations of Non-rigid Molecules*, edited by J. Laane, M. Dakkouri, B. van der Veken, and H. Oberhammer (Kluwer, Dordrecht, The Netherlands, 1993), pp. 391–408.

[35] Y. Abashkin, F. Mele, N. Russo, and M. Toscano, Int. J. Quantum Chem. **52**, 1011 (1994).

[36] A.J. Cox, T.A. Ford, and L. Glasser, J. Mol. Structure (Theochem) **312**, 101 (1994).

[37] J. Sadlej and P. Mazurek, J. Mol. Structure (Theochem) **337**, 129 (1995).

[38] M. Kieninger and O.N. Ventura, J. Mol. Structure (Theochem) **390**, 157 (1997).

[39] J. Sadlej, J. Makarewicz, and G. Chalasinski, J. Chem. Phys. **109**, 3919 (1998).

[40] A.L. Garden, J.R. Lane, and H.G. Kjaergaard, J. Chem. Phys. **125**, 144317 (2006).

[41] J.A. Altmann and T.A. Ford, J. Mol. Structure (Theochem) **818**, 85 (2007).

[42] Y. Tatamitani and T. Ogata, J. Chem. Phys. **121**, 9885 (2004).

[43] T. Ogata and F.J. Lovas, J. Mol. Spectrosc. **162**, 505 (1993).

[44] J.K. Rice, L.H. Coudert, K. Matsumura, R.D. Suenram, F.J. Lovas, W. Stahl, D.J. Pauley, and S.G. Kukolich, J. Chem. Phys. **92**, 6408 (1990).

[45] G.T. Fraser, K.R. Leopold, and W. Klemperer, J. Chem. Phys. **81**, 2577 (1984).

[46] G.T. Fraser, D.D. Nelson, A. Charo, and W. Klemperer, J. Chem. Phys. **82**, 2535 (1985).

[47] L. Fredin and B. Nelander, Chem. Phys. **15**, 473 (1976).

[48] B. Jönsson and B. Nelander, Chem. Phys. **25**, 263 (1977).

[49] M.J. Wojcik, M. Boczar, and T.A. Ford, Chem. Phys. Lett. **348**, 126 (2001).

[50] R.D. Amos, N.C. Handy, P.J. Knowles, J.E. Rice, and A.J. Stone, J. Phys. Chem. **89**, 2186 (1985).

[51] M.J. Frisch, G.W. Trucks, H.B. Schlegel, G.E. Scuseria, M.A. Robb, J.R. Cheeseman, G. Scalmani, V. Barone, B. Mennucci, G.A. Petersson, H. Nakatsuji, M. Caricato, X. Li, H.P. Hratchian, A.F. Izmaylov, J. Bloino, G. Zheng, J.L. Sonnenberg, M. Hada, M. Ehara, K. Toyota, R. Fukuda, J. Hasegawa, M. Ishida, T. Nakajima, Y. Honda, O. Kitao, H. Nakai, T. Vreven, J.A. Montgomery, Jr., J.E. Peralta, F. Ogliaro, M. Bearpark, J.J. Heyd, E. Brothers, K.N. Kudin, V.N. Staroverov, R. Kobayashi, J. Normand, K. Raghavachari, A. Rendell, J.C. Burant, S.S. Iyengar, J. Tomasi, M. Cossi, N. Rega, J.M. Millam, M. Klene, J.E. Knox, J.B. Cross, V. Bakken, C. Adamo, J. Jaramillo, R. Gomperts, R.E. Stratmann, O. Yazyev, A.J. Austin, R. Cammi, C. Pomelli, J. W. Ochterski, R.L. Martin, K. Morokuma, V.G. Zakrzewski, G.A. Voth, P. Salvador, J.J. Dannenberg, S. Dapprich, A.D. Daniels, O. Farkas, J.B. Foresman, J.V. Ortiz, J. Cioslowski, and D.J. Fox, *Gaussian-09, Revision A.02*. (Gaussian, Inc., Wallingford, CT, 2009).

[52] C. Møller and M.S. Plesset, Phys. Rev. **46**, 618 (1934).

[53] T.H. Dunning, Jr., J. Chem. Phys. **90**, 1007 (1989).

[54] R.A. Kendall, T.H. Dunning, Jr., and R.J. Harrison, J. Chem. Phys. **96**, 6796 (1992).

[55] E. Woon and T.H. Dunning, Jr., J. Chem. Phys. **98**, 1358 (1993).

[56] K.A. Peterson, D.E. Woon, and T.H. Dunning, Jr., J. Chem. Phys. **100**, 7410 (1994).

[57] A. Wilson, T. van Mourik, and T.H. Dunning, Jr., J. Mol. Structure (Theochem) **388**, 339 (1997).

[58] B. Liu and A.D. McLean, J. Chem. Phys. **59**, 4557 (1973).

[59] S.F. Boys and F. Bernardi, Mol. Phys. **19**, 553 (1970).

[60] N. Chetty and V.W. Couling, Mol. Phys. **109**, 655 (2011).

[61] R.L. Shoemaker and W.H. Flygare, Chem. Phys. Lett. **6**, 576 (1970).

[62] J.K. Wilmshurst, Can. J. Chem. **38**, 467 (1960).